JACS
JOURNAL OF THE AMERICAN CHEMICAL SOCIETY
Communication
pubs.acs.org/JACS

Generalized Synthesis of Zeolite-Type Metal–Organic Frameworks Encapsulating Immobilized Transition-Metal Clusters

Shou-Tian Zheng,[†] Chengyu Mao,[‡] Tao Wu,[‡] Sangyune Lee,[†] Pingyun Feng,*[,‡] and Xianhui Bu*[,†]

[†]Department of Chemistry and Biochemistry, California State University, Long Beach, California 90840, United States
[‡]Department of Chemistry, University of California, Riverside, California 92521, United States

Supporting Information

ABSTRACT: Zeolites are generally made from tetrahedral nodes and ditopic linkers. Reported here is a versatile method based on trifunctional ligands. With this method, two functional groups are used to form zeolitic nets, while the third one serves to immobilize metal clusters within the channels. The process is driven by the coexistence of multiple inorganic building blocks generated in the heterometallic system. The generality of this method is shown by three distinct metal–organic frameworks mimicking $AlPO_4$-5 (**AFI**) and **BCT** zeotypes as well as the cubic **lcs** topology. The correlation between the framework topology and trapped metal species reveals the unique bidirectional control (framework topology ↔ confined metal species) that may be exploited to create a large family of zeotypes with channels modified by different metal ions and clusters.

Porous materials are attracting increasing attention because of their applications, such as catalysis and gas separation.[1−5] Natural zeolites contain tetrahedral SiO_4 and AlO_4 joined by Si–O–Al (Si) into 3D frameworks. The beautiful and industrially useful zeolite architectures have fascinated generations of scientists and have shaped one of the most fruitful materials design strategies (called the 4-2 method here) based on tetrahedral nodes and bicoordinate (or ditopic) links. This 4-2 strategy has been used to create a large number of zeolite-like materials in compositions from silicates and phosphates to chalcogenides and imidazolates, in conjunction with various tetrahedral nodes from Li and B to In and Sn.[6−18]

The dependence on ditopic links has been so entrenched in the synthesis of four-connected zeotypes that rarely was it perceived as limiting, until we began our efforts to create metal–organic zeolites. Clearly, the reliance on ditopic ligands would restrict us to only a small subset of a large family of available ligands. There is thus a need for strategies (for mimicking zeolite topologies) that can take advantage of diverse organic ligands.

We propose here a general strategy for developing zeolite-type frameworks from polyfunctional ligands by delegating different roles to available functional groups. Two of these functional groups are to be reserved for forming zeolite-type nets, while the remaining ones are left to perform other functions. We illustrate the feasibility of this strategy by using a simple tritopic ligand (1,3,5-benzenetricarboxylic acid, or H_3BTC) and four-connected metal node (In^{3+}) to construct different zeolite-like frameworks.

Specifically, with this method (denoted the 4-2-1 method, 1 refers to the number of hooks per ligand, see below), two functional groups (called framework-forming groups) will cross-link tetrahedral nodes to form zeolite-like nets, while the remaining functional group (called the hook) is used to immobilize other species, such as monomeric and dimeric metal clusters.

Interestingly, each hook does not act alone. Instead, depending on the type of zeolite topology and channel size, two, three, or even four hooks (here, a hook is the third –COO group of a BTC ligand) are positioned and oriented in such a way that they cooperatively capture the same metal ion or cluster, as if a single hook is not strong enough to do the deed. Also, depending on the channel size, the captured metal ions/clusters exhibit site preference, for example, by occupying the off-centered positions to pad the cylindrical wall of large channels or by simply sitting at the center of small channels.

In the context of the topological control of zeolite-like frameworks, we often resort to structure-directing effects of the extra-framework species, such as alkylammonium cations, through electrostatic, H-bonding, or other noncovalent interactions, and more recently, of the noncovalent link–link interactions in zeolitic imidazolate frameworks. In this work, a new mechanism for the control of zeolite topology is in play, which is the structure-directing role of the captured metal ions or clusters through covalent metal–hook interactions.

While still at the nascent stage with few known examples, this 4-2-1 method holds great promise, because it not only allows the formation of zeolite-type frameworks but also provides a versatile path for the modification of frameworks due to the presence of hooks on the framework. Here we report three types of high-symmetry metal carboxylate zeolite-like frameworks, denoted CPM-16-M, CPM-17-M, and CPM-26-M (Table S1; M = Mn, Co, or Ni for CPM-16, M = Co or Zn for CPM-17 and -26, CPM = crystalline porous materials). These materials possess a ring size of 4, 6, 8, or 12 (the ring size refers to the number of tetrahedral nodes in the ring) and exhibit three distinctly different framework topologies with 1D or 3D channel systems.

CPM-16 mimics the $AlPO_4$-5 framework (the zeolite **AFI** net) with unidimensional 12-, 6-, and 4-ring channels (Figure 1). In the large 12-ring channels, a pair of neighboring hooks

Received: May 29, 2012
Published: July 12, 2012

   dx.doi.org/10.1021/ja305181y | J. Am. Chem. Soc. 2012, 134, 11936–11939

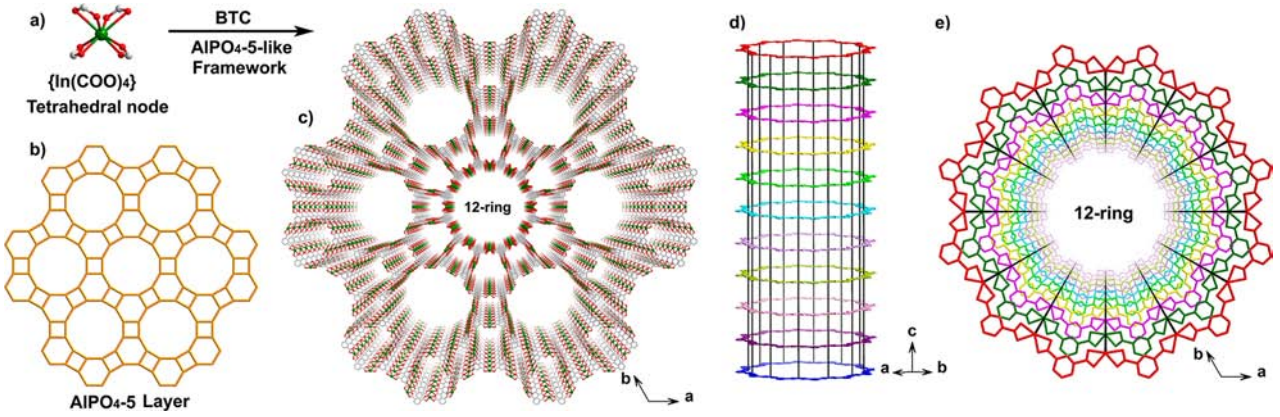

Figure 1. CPM-16 framework: (a) $\{In(COO)_4\}$ tetrahedral node, (b) $AlPO_4$-5 layer, (c) 3D $AlPO_4$-5-like In–BTC framework, and (d,e) side and top views of 12-ring channel.

grab onto a V-shaped $M_2(OH)$ dimer near the wall of the channel, while in the 6-ring channel, a trio of C_3-related hooks act together to immobilize a paddlewheel M_2 dimer at the channel center (Figure 2). CPM-17 with the 4-connected **lcs** topology consists of 3D intersecting 6-ring channels with the paddlewheel dimer (Co_2 or Zn_2) held at the center of the channel by three hooks (Figure 3). Finally, CPM-26 with the **BCT** zeolitic topology consists of 8-, 6-, and 4-ring channels. In contrast with CPM-16 and -17 that use 2/3 and 3 hooks, respectively, CPM-26 uses as many as 4 chelating hooks to trap a single In^{3+} inside the channel as well as using 4 nonchelating hooks to confine a single Zn^{2+} or Co^{2+} within the channel (Figure 4). The correlation between the framework topology/channel size, type of the metal species captured within them, and the mode of the capture reveals a unique type of bidirectional control (framework topology ↔ captured metal species) that may be exploited to further develop this family of materials. Due to the isostructural nature in each series, CPM-16-Co, CPM-17-Co, and CPM-26-Co are chosen for further discussion below.

Insight into the formation and topology of CPM-16-Co can be gained by starting from its multiple inorganic and organic building blocks. There are three types of inorganic building blocks: tetrahedral indium node $\{In(COO)_4\}$ (Figure 1a), hydroxy-bridged V-type cobalt dimer $\{Co_2(OH)(COO)_2(H_2O)_6\}$ (Figure 2a), and paddlewheel cobalt dimer $\{Co_2(COO)_3(H_2O)_2\}$ (Figure 2e). There are three kinds of BTC ligands: one symmetrically bonded to three In^{3+} nodes (**S-BTC**, Figure S1), one unsymmetrically bonded to two In^{3+} nodes, and one $Co_2(OH)$ dimer (**U-BTC1**), and one unsymmetrically bonded to two In^{3+} nodes and one Co_2 dimer (**U-BTC2**). Coassembly of these framework building blocks, together with cationic charge-balancing species and solvent molecules, leads to one of the most beautiful frameworks.

CPM-16-Co bears a great resemblance to $AlPO_4$-5 which is based on the eclipsed stacking of the 3-connected 4.6.12 Archimedean layer (symbol: *fxt*) (Figure 1b). For $AlPO_4$-5 itself, Al and P occupy 3-connected nodes (in the *fxt* layer) with 2-connected oxygen in-between Al and P (i.e., Al–O–P). The adjacent 4.6.12 layers are linked by interlayer oxygens that connect Al and P nodes in the 4.6.12 layer into a 3D $AlPO_4$-5 framework.

In CPM-16-Co, a reverse pattern occurs within the 4.6.12 layer because **S-BTC** ligands occupy the 3-connected nodes (in

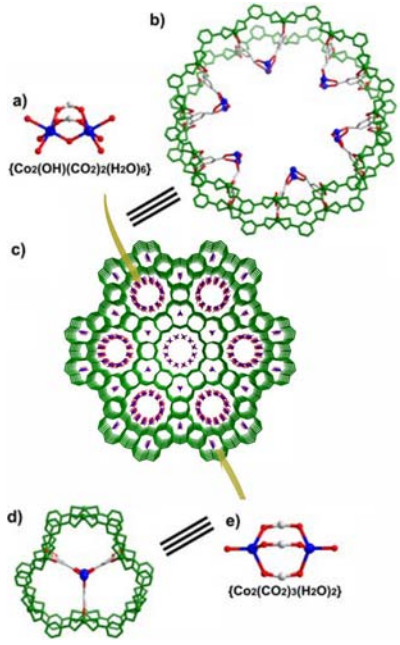

Figure 2. Immobilization of two different dimers in CPM-16-Co: (a) V-type Co dimer, (b) a double 12-ring encapsulating 6 V-type dimers, and (c) 3D framework with Co dimers in both 6- and 12-ring channels. (d) Double 6-rings encapsulating a paddlewheel Co dimer, and (e) paddlewheel Co dimer.

place of Al and P) while In^{3+} ions, playing the role of oxygen in $AlPO_4$-5, join two **S-BTC** ligands in the layer (Figure S2). It is worth noting that all BTC ligands within the 4.6.12 layer are symmetrically bonded to three In^{3+} sites. Since all functional groups of the 3-connected **S-BTC** ligand within the 4.6.12 layer are used up, it is not possible to form regular $AlPO_4$-5 structure by pillaring through 3-connected **S-BTC** nodes in the 4.6.12 layer. Instead, adjacent layers are pillared together by connecting In^{3+} nodes in the 4.6.12 layer with the unsymmetrically bonded BTC ligands (**U-BTC**) (Figure 1c–e). Such interlayer **U-BTC** ligands only need to use two chelating –COO groups to pillar the 4.6.12 layers, with the third functional group left as the hook.

Half of the hooks from interlayer pillaring ligands (**U-BTC2**) point toward the center of 6-ring channels, and these hooks work in groups of three to capture $\{Co_2(COO)_3(H_2O)_2\}$ paddlewheel clusters (Figure 2c,d). The other half of the hooks

dx.doi.org/10.1021/ja305181y | J. Am. Chem. Soc. 2012, 134, 11936–11939

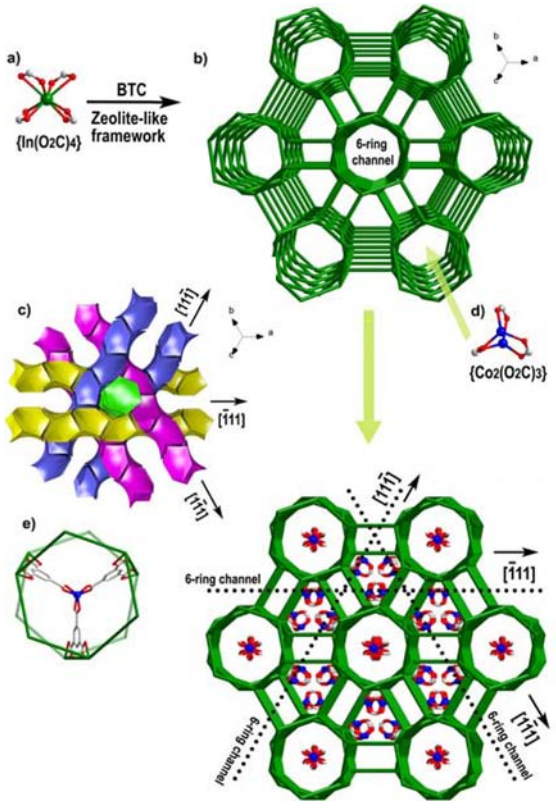

Figure 3. 3D framework in CPM-17-Co and capture of paddlewheel dimers within them: (a) tetrahedral $\{In(COO)_4\}$ node; (b) 3D **lcs**-type net; (c) view of four intersecting channels along [111] (green); [$\bar{1}$11] (yellow), [1$\bar{1}$1] (purple), and [11$\bar{1}$] (blue) directions; (d) $\{Co_2(COO)_3\}$ dimer; (e) section of 6-ring channel, showing a trapped Co dimer; and (f) 3D framework with $\{Co_2(COO)_3\}$ dimers in channels. Dashed lines indicate equivalent channels in three other directions.

(on **U-BTC1**) point toward the center of 12-ring channels, and they work in pairs to capture the V-shaped $\{Co_2(OH)(COO)_2(H_2O)_6\}$ clusters. Because of the large size of 12-ring channels, a total of 6 $Co_2(OH)$ dimers are captured in every double 12-ring (Figure 2b)! The remaining coordination sites on each dimer are completed by solvent molecules. In addition to the Co dimer, other metals, such as Mn and Ni, can also be captured, resulting in a series of metal−organic frameworks (MOFs) (CPM-16-M) containing the same framework with walls padded by various types of metal clusters.

Unlike CPM-16-Co with a mix of **S-BTC** and **U-BTC**, CPM-17-Co has only **U-BTC** (Figure S4a). Each **U-BTC** uses its two framework-forming COO^- groups to bond with In^{3+} ions in a bidentate chelate mode to form a tetrahedral framework with the **lcs** net (Figures 3a,b and S5). The **lcs**-type framework contains only $\{In_6(BTC)_6\}$ 6-rings and has 3D intersecting channels along [111], [$\bar{1}$11], [1$\bar{1}$1], and [11$\bar{1}$] directions (Figure 3c). The third COO^- group of each BTC ligand points toward the center of these channels and coordinates to a Co dimer (Figures 3e and S6) at the center of channels. Similar to Co_2 paddlewheel dimers in 6-ring channels of CPM-16-Co, each Co dimer in CPM-17-Co is also bonded to three COO^- groups from three U-BTC ligands. The difference is that the Co sites in CPM-17-Co have octahedral coordination with remaining coordination sites completed by three solvent molecules (1,3-dimethyltetrahydro-2(1*H*)-pyrimidinone).

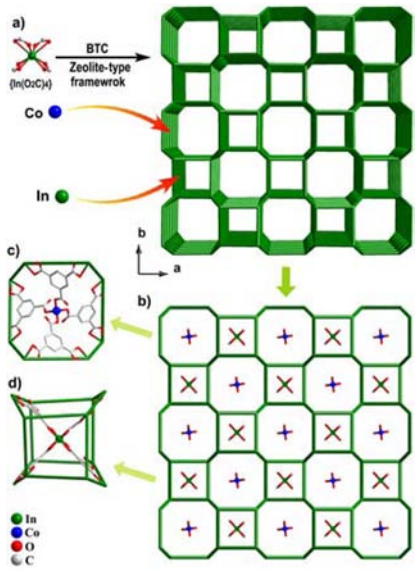

Figure 4. BCT framework in CPM-26 and capture of In^{3+} and Co^{2+} in its channels. (a) **BCT** framework formed from In^{3+} nodes. (b) 3D framework with immobilized Co^{2+} and In^{3+} at the center of 8- and 4-ring channels, respectively. (c) Top view of the "cod-cage" with captured Co^{2+}. (d) Zeolite *lau* cage with captured In^{3+} at the center.

CPM-26-Co mimics a rare mineral zeolite named as Mg-BCTT. Its asymmetric unit consists of two In^{3+} sites (an in-framework In1 and an extra-framework In2), one Co^{2+}, and two BTC ligands (Figure S7). The In1 ions are cross-linked by two carboxyl groups of each BTC to form a 3D framework with zeolitic **BCT** topology originally found in Mg-BCTT with K^+ trapped within the pore (Figure 4a). The BCT topology is formed by eclipsed stacking of rugged hexagonal sheets with $\{In_6(BTC)_6\}$ 6-rings along tetragonal *a* or *b* axes or alternatively by the eclipsed stacking of 4.8.8 layers along the *c*-axis. A key feature of the **BCT** topology is the presence of the $In_{12}(BTC)_{12}$ laumontite cage (*lau*-cage, originally found in the zeolite mineral laumontite, Figure 4d) bounded by two opposite 4-rings and two pairs of opposite 6-rings.

One unique feature in CPM-26 is the simultaneous capture of two different metal species (In^{3+} and Co^{2+}/Zn^{2+}), performed by two sets of four hooks directed toward the center of 4- or 8-ring channels. It takes four hooks in a bidentate chelating mode to capture the "extra-framework" In^{3+} ion at the center of the *lau*-cage lying at the intersection of mutually perpendicular two 6-ring channels and one 4-ring channel. In comparison, each Co^{2+} is anchored at the center of the 8-ring channels by four COO^- groups in a monodentate coordination mode (Figure 4c). Each 8-ring is boat shaped and is denoted here as the "cod-cage" (Figure S8), because it looks like the typical conformation of a common ligand, cycloocta-1,5-diene (cod). With In^{3+} trapped at the center of the *lau*-cage and Co^{2+}/Zn^{2+} immobilized at the center of the "cod-cage", CPM-26 is the first zeolite−MOF with cages and channels covalently decorated by two kinds of ordered metal ions. It is tempting to suggest that single In^{3+} and single Co^{2+} work in synergy to template the formation of the *lau*-cage and "cod-cage", respectively, contributing to the crystallization of CPM-26 with the zeolitic BCT topology.

Loss of solvent molecules in CPM-16-Co, CPM-17-Co, and CPM-26-Co is observed in the temperature range 40−320 °C (Figure S9). Powder X-ray diffraction further suggests that

dx.doi.org/10.1021/ja305181y | *J. Am. Chem. Soc.* 2012, 134, 11936−11939

CPM-16-Co, CPM-17-Co, and CPM-26-Co retain their crystallinity up to approximately 100, 350, and 200 °C, respectively (Figures S10−15). Apparently, the thermal stability is correlated with the size of the largest ring. Permanent porosity of activated samples CPM-16-Co and CPM-17-Co was indicated by CO_2 sorption experiments at 273 K (Figure S16).

In summary, through the synthesis of three series of MOFs (CPM-16, -17, and -26), we demonstrate the general feasibility to construct zeolite-like frameworks from polyfunctional ligands. For the BTC ligand with three geometrically equivalent −COO groups, a key aspect of our strategy is to devise ways to enable −COO groups to bond unsymmetrically to both framework metal nodes and immobilized metal clusters. In this work, this kind of "symmetry-breaking" mode is achieved by employing the heterometallic system that helps to generate various metal ions and clusters with complementary coordination chemistry. The future work will include the exploration of different polyfunctional ligands as well as other heterometallic systems. The need for further exploring this synthetic strategy comes from the potential of this method for the creation of a new generation of zeolite-like materials whose frameworks are decorated with metal centers that may be useful for applications, such as catalysis or adsorption. In addition, this method may provide a path for the pore space partition and optimization through immobilized metal ions or clusters within channels or cages of zeolite-like nets. The possibility of using metal−ligand coordination interactions to template the framework formation and to control its topology, as demonstrated by this work, may have a broad impact in the synthetic design of porous frameworks.

■ ASSOCIATED CONTENT

Supporting Information

Syntheses and characterizations, TGA and XRD, CIF files, and additional structural figures. This material is available free of charge via the Internet at http://pubs.acs.org.

■ AUTHOR INFORMATION

Corresponding Author

xbu@csulb.edu; pingyun.feng@ucr.edu

Notes

The authors declare no competing financial interest.

■ ACKNOWLEDGMENTS

The Research at CSULB was supported by the National Science Foundation under award no. DMR-0846958 (synthesis of samples, crystallographic and topological studies).The research at UCR was supported by the U.S. Department of Energy, Office of Basic Energy Sciences, Division of Materials Sciences and Engineering under award no. DE-SC0002235 (XRD, stability, and gas sorption studies). Acknowledgement is made to the donors of the ACS Petroleum Research Fund for partial support of a portion of the synthetic studies (X.B. 50635-UR10).

■ REFERENCES

(1) (a) Farha, O. K.; Yazaydın, O.; Eryazici, I.; Malliakas, C.; Hauser, B.; Kanatzidis, M. G.; Nguyen, S. T.; Snurr, R. Q.; Hupp, J. T. *Nat. Chem.* **2010**, *2*, 944. (b) Ferey, G.; Serre, C.; Devic, T.; Maurin, G.; Jobic, H.; Llewellyn, P. L.; Weireld, G. D.; Vimont, A.; Daturi, M.; Chang, J. S. *Chem. Soc. Rev.* **2011**, *40*, 550. (c) Kreno, L. E.; Leong, K.; Farha, O. K.; Allendorf, M.; Duyne, R. P. V.; Hupp, J. T. *Chem. Rev.* **2012**, *112*, 1105. (d) Li, J. R.; Zhou, H. C. *Nat. Chem.* **2010**, *2*, 893.

(2) (a) Parnham, E. R.; Morris, R. E. *Acc. Chem. Res.* **2007**, *40*, 1005. (b) Suh, M. P.; Park, H. J.; Prasad, T. K.; Lim, D. W. *Chem. Rev.* **2012**, *112*, 782. (c) Horcajada, P.; Gref, R.; Baati, T.; Allan, P. K.; Maurin, G.; Couvreur, P.; Férey, G.; Morris, R. E.; Serre, C. *Chem. Rev.* **2012**, *112*, 1232.

(3) (a) O'Keeffe, M.; Yaghi, O. M. *Chem. Rev.* **2012**, *112*, 675. (b) Li, J. R.; Sculley, J.; Zhou, H. C. *Chem. Rev.* **2012**, *112*, 869. (c) Sumida, K.; Rogow, D. L.; Mason, J. A.; McDonald, T. M.; Bloch, E. D.; Herm, Z. R.; Bae, T. H.; Long, J. R. *Chem. Rev.* **2012**, *112*, 724.

(4) (a) Sava, D. F.; Rodriguez, M. A.; Chapman, K. W.; Chupas, P. J.; Greathouse, J. A.; Crozier, P. S.; Nenoff, T. M. *J. Am. Chem. Soc.* **2011**, *133*, 12398. (b) Sava, D. F.; Rohwer, L. E. S.; Rodriguez, M. A.; Nenoff, T. M. *J. Am. Chem. Soc.* **2012**, *134*, 3983.

(5) (a) Oliver, S. R. J. *Chem. Soc. Rev* **2009**, *38*, 1868. (b) Fei, H.; Oliver, S. R. J. *Angew. Chem., Int. Ed.* **2011**, *50*, 9066. (c) Lan, Y. Q.; Jiang, H. L.; Li, S. L.; Xu, Q. *Adv. Mater.* **2011**, *23*, 5015. (d) Cui, Y.; Yue, Y.; Qian, G.; Chen, B. *Chem. Rev.* **2012**, *112*, 1126.

(6) (a) Wilson, S. T.; Lok, B. M.; Messina, C. A.; Cannan, T. R.; Flanigen, E. M. *J. Am. Chem. Soc.* **1982**, *104*, 1146. (b) Bekkum, H. V.; Flanigen, E. M.; Jacobs, P. A.; Jansen, J. C. *Introduction to Zeolite Science and Practice*; Elsevier: Amsterdam, The Netherlands, 2001.

(7) (a) Férey, G. *Science* **2001**, *291*, 994. (b) Serre, C.; Millange, F.; Thouvenot, C.; Noguès, M.; Marsolier, G.; Louër, D.; Férey, G. *J. Am. Chem. Soc.* **2002**, *124*, 13519. (c) Férey, G.; Serre, C.; Millange, F.; Surble, S.; Dutout, J.; Margiolaki, I. *Angew. Chem, Int. Ed* **2004**, *43*, 6296.

(8) (a) Cooper, E. R.; Andrews, C. D.; Wheatley, P. S.; Webb, P. B.; Wormald, P.; Morris, R. E. *Nature* **2004**, *430*, 1012. (b) Wheatley, P. S.; Butler, A. R.; Crane, M. S.; Fox, S.; Xiao, B.; Rossi, A. G.; Megson, I. L.; Morris, R. E. *J. Am. Chem. Soc.* **2006**, *128*, 502.

(9) (a) O'Keeffe, M.; Peskov, M. A.; Ramsden, S. J.; Yaghi, O. M. *Acc. Chem. Res.* **2008**, *41*, 1782. (b) Banerjee, R.; Phan, A.; Wang, B.; Knobler, C.; Furukawa, H.; O'Keeffe, M.; Yaghi, O. M. *Science* **2008**, *319*, 939. (c) O'Keeffe, M. *Angew. Chem., Int. Ed.* **2009**, *48*, 8182.

(10) (a) Liu, F. J.; Willhammar, T.; Wang, L.; Zhu, L. F.; Sun, Q.; Meng, X. J.; Carrillo-Cabrera, W.; Zou, X. D.; Xiao, F. S. *J. Am. Chem. Soc.* **2012**, *134*, 4557. (b) Willhammar, T.; Sun, J. L.; Wei, W.; Oleynikov, P.; Zhang, D. L.; Zou, X. D.; Moliner, M.; Gonzalez, J.; Martínez, C.; Rey, F.; Corma, A. *Nat. Chem* **2012**, *4*, 188.

(11) (a) Koh, K.; Wong-Foy, A. G.; Matzger, A. J. *J. Am. Chem. Soc.* **2009**, *131*, 4184. (b) An, J.; Fiorella, R. P.; Geib, S. J.; Rosi, N. L. *J. Am. Chem. Soc.* **2009**, *131*, 8401.

(12) (a) Nouar, F.; Eckert, J.; Eubank, J. F.; Forster, P.; Eddaoudi, M. *J. Am. Chem. Soc.* **2009**, *131*, 2864. (b) Wang, S.; Zhao, T.; Li, G.; Wojtas, L.; Huo, Q.; Eddaoudi, M.; Liu, Y. *J. Am. Chem. Soc.* **2010**, *132*, 18038.

(13) (a) Zhang, Z.; Dai, S.; Hunt, R. D.; Wei, Y.; Qiu, S. *Adv. Mater.* **2001**, *13*, 493. (b) Yan, W.; Bao, L.; Mahurin, S. M.; Dai, S. *Appl. Spectrosc.* **2004**, *58*, 18.

(14) (a) Liao, Y. C.; Liao, F. L.; Chang, W. K.; Wang, S. L. *J. Am. Chem. Soc.* **2004**, *126*, 1320. (b) Liao, Y. C.; Lin, C. H.; Wang, S. L. *J. Am. Chem. Soc.* **2005**, *127*, 9986.

(15) (a) Bu, X. H.; Tong, M. L.; Chang, H. C.; Kitagawa, S.; Batten, S. R. *Angew. Chem., Int. Ed.* **2004**, *43*, 192. (b) Duriska, M. B.; Neville, S. M.; Lu, J.; Iremonger, S. S.; Boas, J. F.; Kepert, C. J.; Batten, S. R. *Angew. Chem., Int. Ed* **2009**, *48*, 8919.

(16) Yan, Y.; Telepeni, I.; Yang, S.; Lin, X.; Kockelmann, W.; Dailly, A.; Blake, A. J.; Lewis, W.; Walker, G. S.; Allan, D. R.; Barnett, S. A.; Champness, N. R.; Schröder, M. *J. Am. Chem. Soc.* **2010**, *132*, 4092.

(17) (a) Huang, X. C.; Lin, Y. Y.; Zhang, J. P.; Chen, X. M. *Angew. Chem., Int. Ed.* **2006**, *45*, 1557. (b) Stylianou, K. C.; Heck, R.; Chong, S. Y.; Bacsa, J.; Jones, J. T. A.; Khimyak, Y. Z.; Bradshaw, D.; Rosseinsky, M. J. *J. Am. Chem. Soc.* **2010**, *132*, 4119.

(18) (a) Zhang, Q.; Bu, X.; Zhang, J.; Wu, T.; Feng, P. *J. Am. Chem. Soc.* **2007**, *129*, 8412. (b) Zheng, S. T.; Bu, J. T.; Li, Y.; Wu, T.; Zuo, F.; Feng, P.; Bu, X. *J. Am. Chem. Soc.* **2010**, *132*, 17062. (c) Zheng, S. T.; Wu, T.; Zuo, F.; Chou, C.; Feng, P.; Bu, X. *J. Am. Chem. Soc.* **2012**, *134*, 1934.